

Video Smoke Detection Based on Multi-feature Fusion and Modified Random Forest

Yuanbin Wang, Qian Han, Yuanyuan Li, and Yujie Li

Abstract—Video smoke detection plays a significant role in real-time fire alarms. In this paper, aiming at the problems of high false positives and high false negatives in complex environments, a video smoke detection algorithm based on multi-feature fusion and modified random forest (RF) is proposed. Firstly, the motion region is detected by ViBe. The noise and holes are processed by morphology. Then, the candidate smoke region is filtered in HSV color space. LBMP, wavelet energy, and smoke growth rate features are extracted from the candidate area. Finally, the multi-features are fused and input into RF classifier for smoke detection. The experimental results show that the modified RF selects the decision trees with high AUC and small correlation through ranking and clustering, which has higher detection accuracy. Furthermore, the proposed method combines the static and dynamic characteristics of smoke, which improves the detection speed effectively and has good robustness. It can avoid high false positives and high false negatives in complex environments.

Index Terms—modified random forest, ViBe, HSV color space, LBMP

I. INTRODUCTION

FIRE is one of the most common and threatening disasters to public safety. In the early stage of fire, it is often accompanied by smoke. Therefore, smoke detection is beneficial for early fire alarm. Conventional smoke detection mainly relies on sensor equipment. It is easily subject to the surrounding environment, which significantly limits its application scope. With the development of computer vision, video smoke detection has been widely studied [1], [2], [3].

Smoke detection algorithms are mainly divided into conventional algorithms and deep learning algorithms. There are three main parts for conventional methods: moving target extraction, smoke feature extraction, and classification. Zheng Huaibing [4] and Kim [5] et al. employed a Gaussian mixture model to extract smoke area, which determined the basis for feature extraction. Wang Sen et al. [6] used the ViBe

algorithm to extract moving targets. The algorithm has fast computation speed and stable processing effect on illumination change and camera shake. The Optical flow segmentation method can also extract the moving image. However, the calculation is complicated and has not good robustness to noise. In recent years, conventional smoke detection methods mainly focused on the extraction of smoke features and the selection of classifiers. Smoke features are mainly concentrated in color, motion, and texture features. Dong Lanfang et al. [7] extracted the local binary pattern, which describes the texture characteristics and used SVM for classification. Emmy et al. [8] analyzed wavelet frequency and dynamic texture features to determine the smoke area and introduced the gray level co-occurrence matrix (GLCM) to capture the connection between pixels. After extracting the color and shape features, Zhou et al. [9] extracted color and shape features, and proposed pixel variance as texture features according to the lack of wildfire smoke texture features. Ding Huaidui et al. [10] put forward a method based on motion block tracking. Characteristics such as direction and gray attenuation were analyzed. Since the dynamic characteristics have good robustness, the non-smoke blocks were eliminated effectively, and the false-positive rate was reduced. Pundir et al. [11] obtained smoke features by combining RGB and YCbCr color model, but the color of smoke was easily disturbed by fog and moving objects, so it was still tricky for smoke detection. Tong Bobing et al. [12] utilized discrete cosine transform and discrete wavelet transform to extract features, which improved the accuracy of smoke detection. However, the detection effect was not good enough in the complex environment. Liu Kai et al. [13] employed AdaBoost to reduce the false-positive rate and false-negative rate effectively. Dimitropoulos et al. [14] proposed a multi-feature classification method based on SVM, in which more smoke features were employed and more complicated than other methods. Wu Dongmei et al. [15] adopted BP neural network to fuse and judge the dynamic characteristics. The static features and dynamic features were combined, and the accuracy of smoke detection was improved. Compared with conventional methods, deep learning algorithms have better performance. The most representative convolutional neural network (CNN) can automatically extract the essential features of smoke without selecting a classifier, which can avoid the error caused by manual extraction. Li Peng et al. [16] proposed a video smoke detection method based on the Gaussian mixture model and CNN. First, the Gaussian mixture model was employed to extract the moving target, and then the CNN model was applied to smoke detection. Chen Junzhou et al. [17] proposed a CNN framework combining static and dynamic features, which effectively avoided the interference in

Manuscript received October 27, 2020; revised June 29, 2021. This work (Grants 61703329) was supported by the National Natural Science Foundation of China and the National Key Research and Development Program of Shaanxi Province, China(2019KW-046).

Yuanbin Wang is an Associate Professor of Electrical and Control Engineering, Xi'an University of Science and Technology, Xi'an 710054, China (e-mail: 13379232752@163.com).

Qian Han is a Master's degree candidate of Electrical and Control Engineering, Xi'an University of Science and Technology, Xi'an 710054, China (e-mail: 947674382@qq.com).

Yuanyuan Li is a Master's degree candidate of Electrical and Control Engineering, Xi'an University of Science and Technology, Xi'an 710054, China (e-mail: 2764845392@qq.com).

Yujie Li is a Master's degree candidate of Electrical and Control Engineering, Xi'an University of Science and Technology, Xi'an 710054, China (e-mail: 1678931975@qq.com).

complex scenes. Xu et al. [18] used generative adversarial network (GAN) to synthesize smoke images, and trained them together with real smoke images. Although the false detection rate can be reduced, the distribution deviation between the synthetic smoke image and the real image will affect the detection performance to a certain extent. While the neural network is a hot topic, smoke detection depends on substantial data sets and requires many convolution and pooling calculations. Therefore, it is not suitable for the scene with low processing power.

In order to improve the detection accuracy in complex scenes and reduce the false-positive and false-negative rate, we propose a video smoke detection algorithm based on multi-feature fusion and modified random forest, and it has the following advantages: (1) ViBe algorithm can extract the motion area quickly and adapt to the complex environment; (2) LBMP dynamic feature, wavelet energy feature, and smoke growth rate feature are extracted, which has good robustness in the complex environment; (3) The modified RF selects trees with strong classification ability and small correlation, which improves the detection accuracy and reduces the false-negative rate. The schematic diagram is shown in Fig. 1.

II. SUSPECTED SMOKE AREA DETECTION

A. Motion area detection

ViBe is a motion detection algorithm based on pixel-level modeling [19], which can deal with illumination variation stably, and has the characteristics of high speed and a small amount of calculation. Firstly, the pixel value of the x point in the first frame is $V(x)$, and N pixel values are selected from the neighborhood randomly as the sample set $M(x) = \{v_1, v_2, \dots, v_N\}$ of pixel x . Then, the foreground detection is performed by comparing the pixel value in a video sequence with the historical value of the background model. The formula is as follows

$$\#\{S_R(v(x)) \cap M(x)\} > \#min \quad (1)$$

Where $\#min$ is the threshold value, generally set to 2, S_R represents the number of pixels whose distance between the video frame and pixel value of the sample set is less than R . When S_R is larger than the threshold, it is classified as a

background pixel. To make the background model adapt to the change of illumination and moving objects, we adopt the conservative update strategy and random sampling method [20]. The updated strategy ensures that the foreground pixels will not fill the background model, while random sampling can avoid image ghost effectively.

Isolated noises, small gaps, and holes may exist in the detected motion areas. To extract the motion areas completely, we used morphological methods to analyze the connected area. Suppose that O is the object to be processed, S is the structural element and used to perform the open and close operation on O . The formula is

$$OPEN(O, S) = (O \odot S) \oplus S \quad (2)$$

$$CLOSE(O, S) = (O \oplus S) \odot S \quad (3)$$

Where \odot is the erosion operation, \oplus is the expansion operation. Firstly, the image is processed by open operation, and then the gaps and holes in the image are filled by closed operation after the noise is eliminated.

B. Filtering in HSV color space

Although motion detection algorithm can detect candidate smoke areas, it may contain other non-smoke moving objects, such as pedestrians and vehicles. It is indispensable to remove the non-smoke movement area to improve detection accuracy and reduce the false-positive rate. In the early stage, the color of smoke is primarily white or gray-white, we can only analyze and detect white and gray-white smoke. The HSV color space can avoid the threshold division problem caused by the high correlation of the RGB space, so the image is filtered in the HSV space. By looking up the table, the H component threshold is from 0 to 180, the S component threshold component is from 0 to 43, and the V threshold component is 46 to 255. HSV color space filter is shown in Fig. 2 and morphological experiment in four different scenes of smoke videos is shown in Fig. 3.

III. FEATURE EXTRACTION OF SMOKE

Most interferences can be eliminated by the above steps, but it is not enough for smoke detection. In view of the dynamic features of smoke, we extracted LBMP, growth rate dynamic feature and wavelet static energy feature. Then, dynamic and static features are combined for smoke detection.

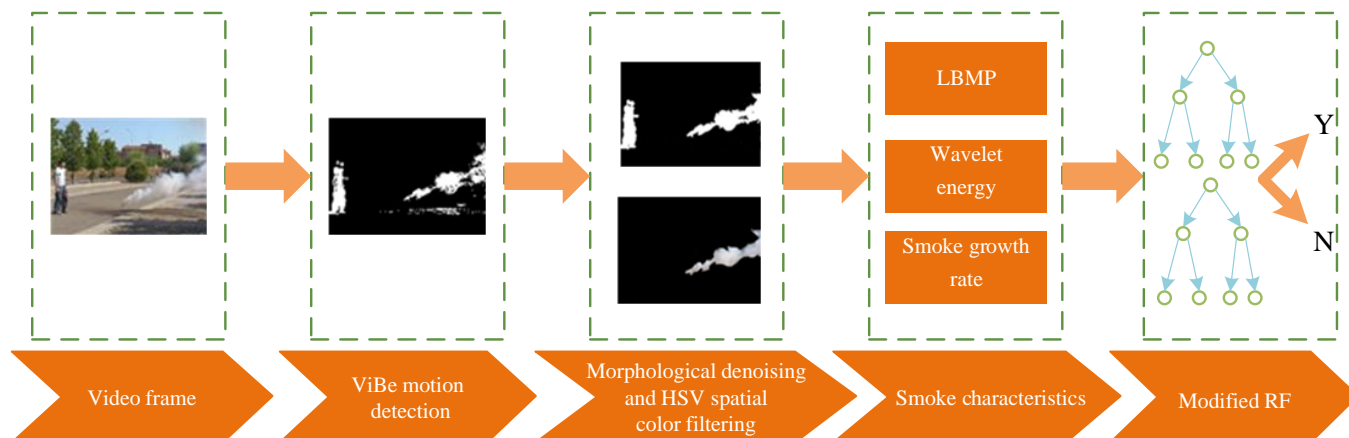


Fig. 1. Schematic diagram of the proposed algorithm

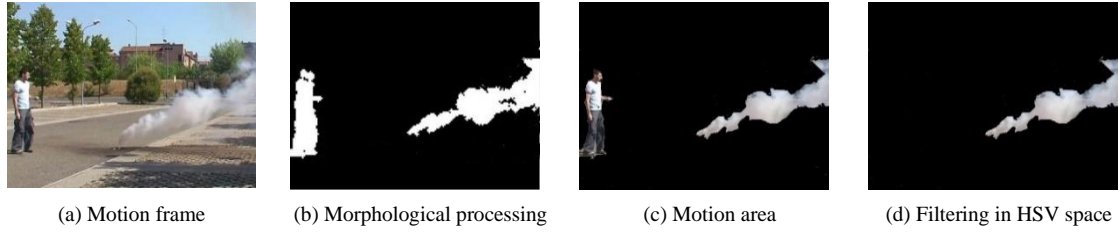


Fig. 2. Filtering in HSV color space

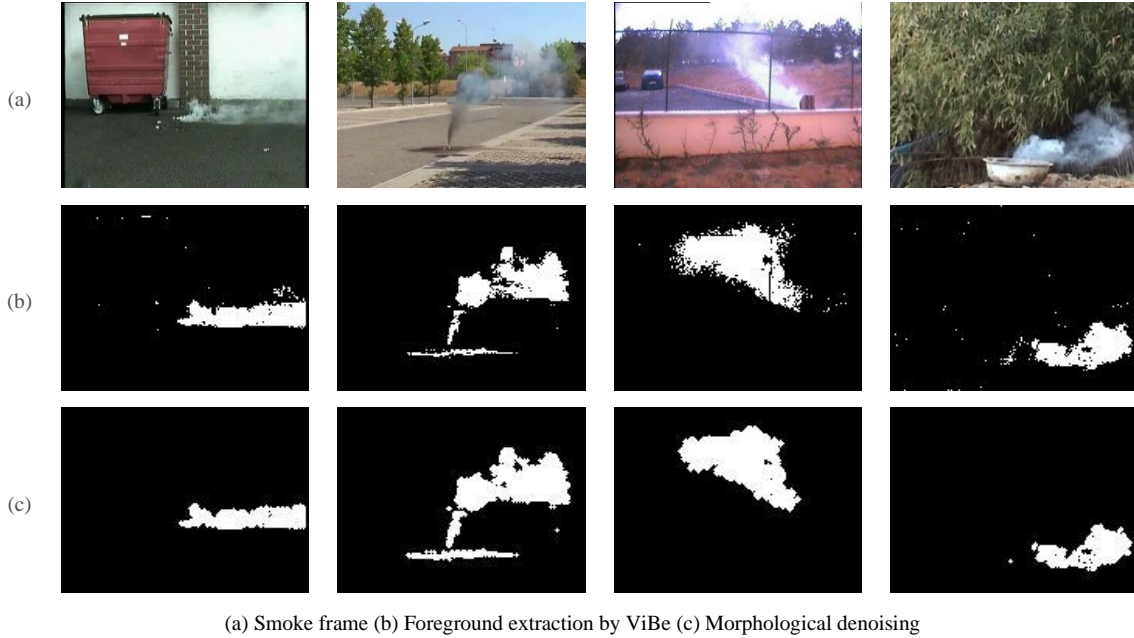


Fig. 3. Extraction and processing of moving smoke

A. LBMP dynamic texture feature

LBMP feature reflects the dynamic characteristics of smoke, which is improved based on the LBP algorithm. The original LBP describes the local texture characteristics of the image [21]. It is expressed as follows

$$LBP_{P,R} = \sum_{p=0}^{P-1} s(g_p - g_c) 2^p \quad (4)$$

$$s(x) = \begin{cases} 1, & x \geq 0 \\ 0, & \text{else} \end{cases} \quad (5)$$

Where g_c is the gray value of the center pixel, P is the number of surrounding pixels, R is the neighborhood radius, and the distance between the center pixel and the neighborhood pixel is Euclidean distance. When LBMP dynamic texture is extracted, the video frame is divided into ten sample blocks, and the search window size is set to 5×5 . Then, LBP value of each pixel is calculated one by one, and the dynamic texture features are calculated by the block matching method. The formula is

$$LBMP(x, y, t) = \min |LBP(P_0) - LBP(P_x)| \quad (6)$$

Where $LBMP(x, y, t)$ is the dynamic information of each pixel, P_x and P_0 correspond to the pixel of the current frame and previous frame in the search window, respectively. For better statistical classification, histogram of LBMP dynamic texture feature is defined as

$$H_i = \sum_{x,y,t} E(LBMP(x, y, t), i) \quad (7)$$

$$E(x, y) = \begin{cases} 1, & LBMP(x, y, t) = i \\ 0, & LBMP(x, y, t) \neq i \end{cases} \quad (8)$$

Where $E(x, y)$ is the variable number of statistical position and i is the search window size. The LBMP feature histogram is obtained based on the smoke frame in Fig. 3, as shown in Fig. 4.

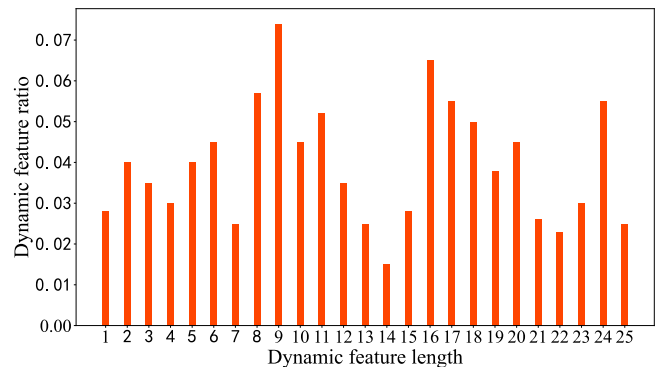


Fig. 4. LBMP dynamic feature histogram

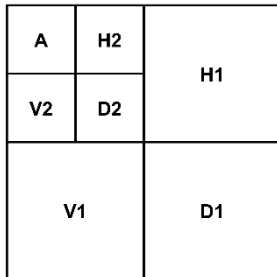
It can be seen from Fig. 4, that the length of the partial dynamic feature of the LBMP sample block is 25, which is determined by the size of the search window. Since each video frame is divided into ten sample blocks, each dynamic texture sequence is represented by ten feature histograms. Therefore, 250 feature vectors are used to describe the dynamic texture features of the smoke video.

B. Wavelet energy feature

Smoke is composed of tiny particles. When the smoke concentration reaches a certain level, the smoke edge become blurry. The high-frequency components of the smoke edge information can be extracted by wavelet decomposition. Firstly, the candidate smoke area is decomposed by one layer of wavelet. Horizontal detail sub-image $H1$, diagonal detail sub-image $D1$ vertical detail sub-image $V1$, and low-resolution image $L1$ are obtained. Then, the energy of low-frequency and high-frequency are calculated according to the decomposed sub-image [22]. The calculation formula is as follows

$$\begin{cases} E_1 = \sum_{i,j} H_k(i,j)^2 \\ E_2 = \sum_{i,j} D_k(i,j)^2 \\ E_3 = \sum_{i,j} V_k(i,j)^2 \\ E_4 = \sum_{i,j} L(i,j)^2 \end{cases} \quad (10)$$

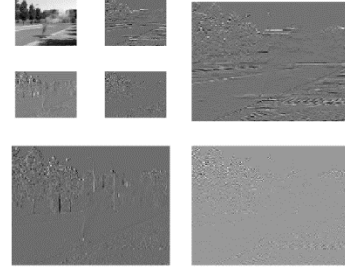
Where E_1 , E_2 , and E_3 are the energy of high-frequency components in the horizontal, diagonal, and vertical direction, respectively. E_4 is a low-frequency component, and k is the k -th wavelet decomposition. In this paper, the $db4$ wavelet is selected as the basis function. With the increment of decomposition series, more image information can be obtained, which provides decisive criteria for subsequent detection. Wavelet decomposition of the smoke frame is shown in Fig. 5. $H2$, $V2$, and $D2$ are high-frequency sub-images after the second layer decomposition, A is the low-frequency part of the second decomposition. (c) is the second level decomposition of (b). After decomposition, horizontal, vertical and diagonal directions of the original image contain two high-frequency energy information, respectively. Six-high frequency energy information and one low-frequency energy information are adopted as a feature vector.



(a) Wavelet two-layer decomposition



(b) Original image



(c) Wavelet transform decomposition

Fig. 5. Schematic diagram of wavelet transform

C. Smoke growth rate feature

Smoke motion has the characteristics of diffusion and growth [23]. For the moving smoke in continuous video frames, the smoke growth rate area can be obtained by the equation:

$$g = \frac{S_{t+\Delta t} - S_t}{(t+\Delta t) - t} \quad (11)$$

Where g is the growth rate, S_t and $S_{t+\Delta t}$ represent the smoke area in frame t and $(t + \Delta t)$, respectively. The growth rate is the change rate of a smoke area with time. We can obtain the growth rate by dividing the pixel number according to the sampling interval.

IV. RANDOM FOREST CLASSIFIER

After the smoke features are extracted, we need to select a classifier to process the features. Conventional classifiers include Support Vector Machine (SVM) [24], BP neural network [25], [26], decision tree and so on. In this paper, the RF classifier is selected for classification because of its high prediction accuracy and excellent robustness. To further improve the detection accuracy, we modified the RF algorithm. The three above smoke features are taken as the input of the classifier.

A. Conventional random forest

The principle of RF algorithm is to randomly select a subset of different training samples and increase the correlation of classification model, so that the model has a stronger generalization ability and can avoid overfitting effectively [27]. The RF algorithm mainly includes training and classification. In the training stage, multiple data sets are extracted by bootstrap randomly. Then, some features are extracted from the data set, and the CART algorithm generates the decision tree. Suppose that the k -th sample ratio in a given data set D is p_k , CART uses the Gini coefficient to divide the attributes. When attribute a is divided from the attribute set, the formula is

$$Gini(D) = 1 - \sum_{k=1}^K p_k^2 \quad (12)$$

$$Gini(D, a) = \sum_{v=1}^V \frac{|D^v|}{|D|} Gini(D^v) \quad (13)$$

Where the smaller the $Gini(D)$, the higher the purity of the data set. V is the number of potential values for discrete attribute a . The attribute with the smallest Gini coefficient can be regarded as the optimal division attribute from the above.

The classification process is to perform voting statistics on each decision tree and obtain the final classification. It is expressed as

$$H(x) = \arg \max_Y \sum_{i=1}^K I_i(x) \quad (H_i(x) = Y) \quad (14)$$

Where $H(x)$ is the final classification result, $H_i(x)$ represents the classification result by a single decision tree model, Y is the output variable, and I is the indicative function.

In general, the classification accuracy of RF algorithm is related to two factors: (1) The correlation between any two trees in the forest. The better the independence between any trees, the smaller the correlation. It will make the model more robust to abnormal points and make the error rate lower. (2) The classification ability of each tree in the forest. The stronger the classification ability of each tree, the lower the error rate of the forest. Because the conventional RF only extracts the data set to generate a decision tree, the factors between the decision trees can be modified to improve the effectiveness of the algorithm.

B. Modified random forest

In view of the two above factors in conventional RF, a modified RF is established to enhance the performance by selecting decision trees with a small correlation and strong classification ability. Firstly, a large number of decision trees are generated according to the smoke characteristics. Then, we choose trees with a high Area Under Curve (AUC), which means the classification ability. It is the area covered by the Receiver Operating Characteristic (ROC) curve and the evaluation indicator of the two-classification model. Finally, the AUC of the decision trees are calculated and sorted from high to low, which shows that the former trees have better classification ability. Usually, the number of selections is set to 50 to 80 percent of all trees. The abscissa and ordinate of AUC are calculated as follows

$$FPR = \frac{FP}{FP+TN} \quad (15)$$

$$TPR = \frac{TP}{TP+FN} \quad (16)$$

Where FPR is the false-positive rate, TPR is the true-positive rate. FP, TN, TP, and FN are the false positive, true negative, true positive, and false negative in the confusion matrix.

To make the correlation between any decision tree small, we calculate the similarity of the decision trees based on Petra Perner [28]. Firstly, the two decision trees are converted to two rule-sets, and the rules are ranked according to the number of attributes n in the rule-set. Then, all the rules are decomposed into sub-rules, and the set of sub-rules is applied to compare the similarity $sim_{i,j}$ of the two decision trees. It is expressed as the following

$$Sim_{i,j} = \frac{1}{n} (Sim_1 + Sim_2 + \dots + Sim_k + \dots + Sim_n) \quad (17)$$

Where $n = \max\{n_i, n_j\}$, Sim_k is the similarity of two sub-rules with the same number of nodes in rule i and j , n_i , n_j represent the number of sub-rules in rule i and j , respectively. The similarity matrix Sim can be constructed as

$$\begin{bmatrix} 1 & Sim_{1,2} & Sim_{1,3} & \dots & Sim_{1,P} \\ Sim_{1,2} & 1 & Sim_{2,3} & \dots & Sim_{2,P} \\ \vdots & \vdots & \vdots & \ddots & \vdots \\ Sim_{P,1} & Sim_{P,2} & Sim_{P,3} & \dots & 1 \end{bmatrix} \quad (18)$$

After obtaining the similarity matrix, k -means clustering is applied to obtain the classification with small correlation. After the classification is completed, the decision trees with the highest AUC are selected from each category. Consequently, decision trees with strong classification ability and small correlations are obtained, and the modified RF model is established by combining the decision trees. The specific steps are as follows

(1) Conventional RF is used to generate K decision trees and sort them according to AUC, denoted as $\{d_1, d_2, \dots, d_K\}$;

(2) Select P decision trees with high AUC from the ranked decision trees (P is set to the first 50%-80% of K trees). That is, the decision trees have strong classification ability;

(3) According to the similarity relationship between decision trees, the rule-set of P decision trees is transformed, and the similarity matrix Sim is obtained;

(4) The similarity matrix Sim is used to cluster P decision trees by K-means, and S categories are obtained (S is taken as $\frac{P}{2}$ by experiments). Then, the decision trees with the highest AUC are selected from the S categories, which have the performance of small correlation and strong classification ability;

(5) Finally, a modified RF classifier is obtained by integrating the selected S decision trees.

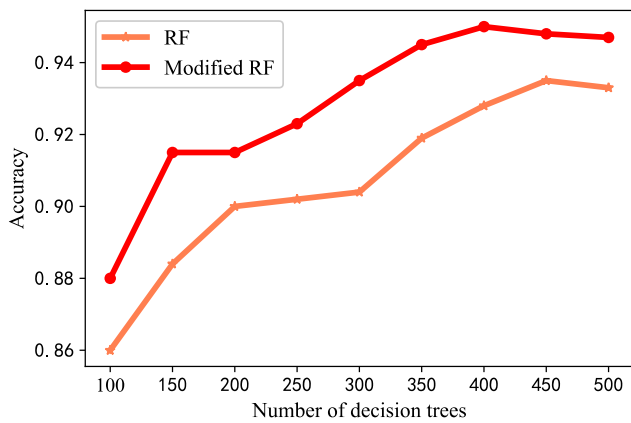
After the classifier is constructed according to the above process, the static and dynamic features extracted are employed as sample data for training. When the classifier is trained, smoke detection can be performed.

V. ANALYSIS OF EXPERIMENTAL RESULTS

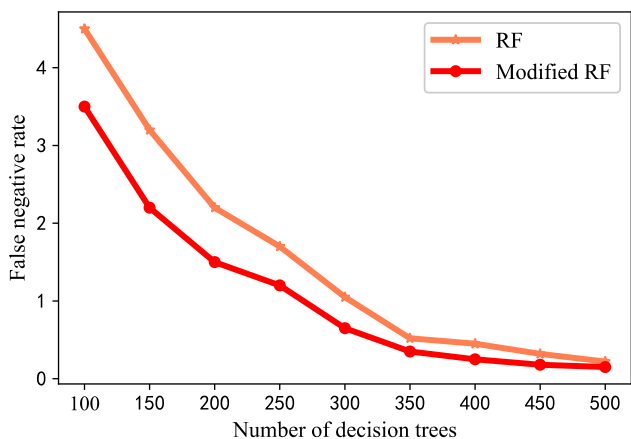
The performance of the algorithm is evaluated by static samples and multi-scene video classification experiments. 6500 positive smoke samples and 2500 negative samples are included. Firstly, foreground extraction and HSV color space filtering are carried out on the smoke video. When the candidate smoke area is obtained, LBMP, wavelet energy, and smoke growth rate features are extracted. Then the number of decision trees 50, 100, 150, and 500 are selected. Conventional and modified RF models are established, respectively. For the modified RF model, P is taken as $\frac{2}{3}$, that is, the first $\frac{2}{3}$ decision trees with higher AUC value and the number of clusters S is $\frac{P}{2}$. The accuracy rate can evaluate the performance of the model. The formula is

$$Accuracy = \frac{TP+TN}{TP+TN+FP+FN} \quad (19)$$

When the number of decision trees is different, the performance evaluation of conventional RF and modified RF models is carried out. Fig. 6. shows the experiment results.



(a) Comparison of accuracy with different decision trees



(b) Comparison of false-negative rate with different decision trees

Fig. 6. Performance evaluation of conventional and modified RF algorithm

From Fig. 6, it can be found that the modified RF is better than conventional RF in the classification effect, and the accuracy rate is increased by 2% on average. With the number rising of decision trees, the false-negative rate gradually decreases. When the decision tree is 400, the detection accuracy and false-negative rate are excellent, so the optimal number is 400. In addition, SVM and BP neural network were applied to compare with them, and the data were selected from the existing smoke data set 1 and set 2, respectively. The data sets size were 4500, and the results were as shown in Fig. 7.

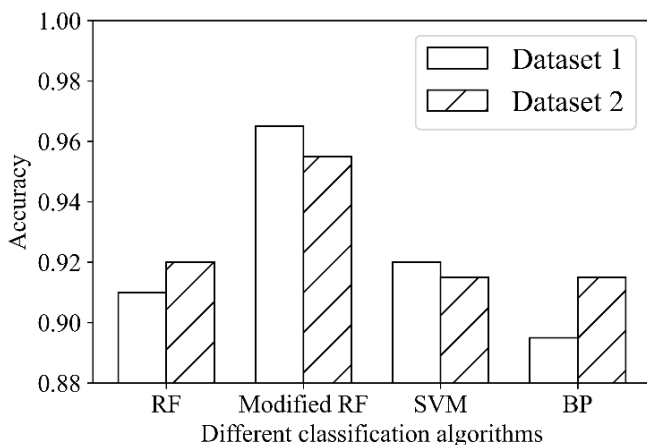


Fig. 7. Comparison between different algorithms

Compared to the four experimental results, the performance of the modified RF algorithm is the best, and there is no apparent difference between SVM and conventional RF. However, the performance of the BP neural network is not as good as the other three algorithms.

To evaluate the proposed algorithm's performance, we compared the reference [13] in the multi-scene video. In reference [13], LBP features and wavelet energy were extracted and classified by AdaBoost, and the performance was excellent in the complex environment. The result in different scenes is shown in Fig. 8. Table I shows the first alarm of 8 smoke videos, Table II shows the false detection of 4 non-smoke videos.

According to the analysis of Table I and II, the first alarm of the proposed algorithm is earlier than that of reference [13]. The former can detect the smoke more quickly, and the number of false positives is less, which can solve the problem of high false positives effectively in complex environment. Based on the two random selections of conventional RF, the proposed algorithm selects the decision tree with strong classification ability and small correlation, and it has better stability in the complex environment.



Fig. 8. Experimental video scene

TABLE I
SMOKE VIDEO EXPERIMENT RESULTS

Number	Video description	Smoke frame appears	First smoke alarm frame	
			Reference [13]	Proposed
1	No wind, close-distance, dense smoke, and fast spread	157	163	161
2	Little wind, close-distance, thinner smoke, fast spread	78	87	83
3	Little wind, long-distance, thinner smoke, rapid spread	134	141	140
4	No wind, close-distance, dense smoke, slow spread	126	134	135
5	No wind, close-distance, dense smoke, fast spread	95	110	106
6	Little wind, close-distance, dense smoke, rapid spread	184	195	190
7	Strong wind, short-distance, thinner smoke, slow spread	150	155	152
8	No wind, short-distance, dense smoke, slow spread	152	156	156

TABLE II
NON-SMOKE VIDEO EXPERIMENT RESULTS

Number	Video description	Alarm times	
		Reference [13]	Proposed
1	Driving car	5	0
2	Leaves shaking	1	0
3	Leaves shaking and people walking around the court	6	1
4	Pavement	0	0

VI. CONCLUSION

A video smoke detection algorithm based on multi-feature fusion and modified random forest is proposed, which uses ViBe motion detection and HSV color space filtering to determine the candidate smoke area. Furthermore, the static and dynamic features of smoke are fused to improve the robustness in the complex environment. In addition, aiming at the correlation and classification ability, a modified RF is constructed, and high-performance decision trees are selected to improve the detection accuracy. The experimental results of the static sample classification show that the proposed method has lower false-positive and false-negative rates than the existing smoke detection algorithms. The experimental results in complex environments show that the proposed method can detect smoke accurately and quickly, and has good robustness. It can be used in indoor and outdoor smoke detection or forest fire prediction.

References

- [1] Shi Jinting, Yuan Feiniu, and Xia Xue, "Video smoke detection: a literature survey," *Journal of Image and Graphics*, vol. 23, no. 3, pp. 303-322, 2018.
- [2] Li Juhu, Fan Ruixian, and Chen Zhibo, "Forest fire image recognition based on color and texture features," *Journal of South China University of Technology*, vol. 48, no. 1, pp. 70-83, 2020.
- [3] Lin G, Zhang Y, Zhang Q, and Jia Y, "Smoke detection in video sequences based on dynamic texture using volume local binary patterns," *Ksii Transactions on Internet & Information Systems*, vol. 11, no. 11, pp. 5522-5536, 2017.
- [4] Zheng Huaibing and Zhai Jiyun, "Forest fire smoke detection based on video analysis," *Journal of Nanjing University of Technology*, vol. 39, no. 6, pp. 686-691, 2015.
- [5] Kim H, Ryu D, and Park J, "Smoke detection using GMM and Adaboost," *International Journal of Computer and Communication Engineering*, vol. 3, no. 2, pp. 123-126, 2014.
- [6] Wang Sen, Ge Siluo, and Zou Jianhua, "Video smoke detection based on color and shape features," *Journal of Computer Applications*, vol. 36, no. 2, pp. 168-170, 2016.
- [7] Dong Lanfang and Yu Jiakui, "Smoke detection method in video based on image separation," *Computer Engineering*, vol. 41, no. 9, pp. 251-254+260, 2015.
- [8] C. Emmy Prema, S. S. Vinsley, and S. Suresh, "Multi-feature analysis of smoke in YUV color space for early forest fire detection," *Fire Technology*, vol. 52, no. 5, pp. 1319-1342, 2016.

- [9] Zhou Z, Shi Y, and Gao Z, "Wildfire smoke detection based on local extremal region segmentation and surveillance," *Fire Safety Journal*, vol. 85, no. 10, pp. 50-58, 2016.
- [10] Ding Huaidui, Liu Shenyou, Xu Yukun, and Wang Wenwei, "Novel video smoke observation and detection method based on the motion track block," *Journal of Safety and Environment*, vol. 16, no. 4, pp. 96-100, 2016.
- [11] Pundir A S and Raman B, "Deep belief network for smoke detection," *Fire Technology*, vol. 53, no. 6, pp. 1-18, 2017.
- [12] Tong Bobing and Wang Shitong, "Video smoke detection using two-level classification algorithm," *Computer Science*, vol. 42, no. 3, pp. 301-306, 2015.
- [13] Liu Kai, Liu Xiang, Chang Liping, Chen Bin, and Wu Zhefu, "Video smoke detection based on YUV color space and multiple feature fusion," *Chinese Journal of Sensors and Actuators*, vol. 32, no. 2, pp. 237-243, 2019.
- [14] Dimitropoulos K, Barmpoutis P, and Grammalidis N, "Higher order linear dynamical systems for smoke detection in video surveillance applications," *IEEE Transactions on Circuits and Systems for Video Technology*, vol. 27, no. 5, pp. 1143-1154, 2017.
- [15] Wu Dongmei, Li Baiping, Wang Nana, He Rong, and Shen Yan, "Smoke detection based on multi-feature fusion," *Journal of Graphics*, vol. 36, no. 4, pp. 587-592, 2015.
- [16] Li Peng and Zhang Yan, "Video smoke detection based on Gaussian mixture model and convolutional neural network," *Laser & Optoelectronics Progress*, vol. 56, no. 21, pp. 140-146, 2019.
- [17] Chen J Z, Wang Z J, Chen H H, and Zuo L Y, "Dynamic smoke detection using cascaded convolutional neural network for surveillance videos," *Journal of University of Electronic Science and Technology of China*, vol. 45, no. 6, pp. 992-996, 2016.
- [18] Xu Gao, Zhang Yongming, Zhang Qixing, Lin Gaohua, and Wang Jinjun, "Deep domain adaptation based video smoke detection using synthetic smoke images," *Fire Safety Journal*, vol. 93, no. 10, pp. 53-59, 2017.
- [19] Barnich, Olivier and M. Van Droogenbroeck, "ViBE: A powerful random technique to estimate the background in video sequences," *IEEE International Conference on Acoustics*, 2009.
- [20] Barnich, Olivier and M. Van Droogenbroeck, "ViBe: A universal background subtraction algorithm for video sequences," *IEEE Transactions on Image Processing*, vol. 20, no. 6, pp. 1709-1724, 2011.
- [21] Badal Soni, Pradip K. Das, and Dalton Meitei Thounaojam, "Dual system for copy-move forgery detection using block-based LBP-HF and FWHT features," *Engineering Letters*, vol. 26, no.1, pp171-180, 2018.
- [22] Sun Jiankun and Yang Ruoyu, "Smoke detection in video based on color histogram and wavelets," *Computer Science*, vol. 41, no. 12, pp. 251-254+287, 2014.
- [23] Li Mingming, "Video smoke detection method based on variational level set image segmentation," *Journal of Jilin University (Information Science Edition)*, vol. 37, no. 6, pp. 701-708, 2019.
- [24] Lan Zhang, Lina Luo, Lei Hu, and Maohua Sun, "An SVM-based classification model for migration prediction of Beijing," *Engineering Letters*, vol. 28, no.4, pp. 1023-1030, 2020.
- [25] Li Wu, Jing Zhou, and Zhouhong Li, "Applying of GA-BP neural network in the land ecological security evaluation," *IAENG International Journal of Computer Science*, vol. 47, no.1, pp. 11-18, 2020.
- [26] Stefanus Santosa, R. A. Pramunendar, D. P. Prabowo, and Yonathan P. Santosa, "Wood types classification using back-propagation neural network based on genetic algorithm with gray level co-occurrence matrix for features extraction," *IAENG International Journal of Computer Science*, vol. 46, no.2, pp. 149-155, 2019.
- [27] Breiman L. "Random Forests," *Machine Learning*, vol. 45, no. 1, pp.5-32, 2001.
- [28] Perner, P, "How to compare and interpret two learnt decision trees from the same domain," *International Conference on Advanced Information Networking & Applications Workshops*, 2013.